A HIGH SPEED, DIGITAL, X-BAND PHASE SHIFTER

by

DOUGLAS HARLAN CORTELYOU

S.B., Massachusetts Institute of Technology
(1964)

SUBMITTED IN PARTIAL FULFILLMENT OF THE
REQUIREMENTS FOR THE DEGREE OF
MASTER OF SCIENCE

at the

MASSACHUSETTS INSTITUTE OF TECHNOLOGY
September 1965

Signature of Author _____
Department of Electrical Engineering, August 23, 1965

Certified by _____
Thesis Supervisor

Accepted by _____
Chairman, Departmental Committee on Graduate Students

A HIGH SPEED, DIGITAL, X-BAND PHASE SHIFTER

by

DOUGLAS HARLAN CORTELYOU

Submitted to the Department of Electrical Engineering on August 23, 1965, in partial fulfillment of the requirements for the degree of Master of Science.

ABSTRACT

This thesis concerns the development of a high speed digital, X-band phase shifter designed to operate at power levels of less than 100 mw over a bandwidth of less than 10KHz. Phase shifting is accomplished by six binary phase shifting elements incorporated in microwave circuitry that adds the phase shifts of the individual elements.

Phase shifts of π, $\pi/2$, $\pi/4$, $\pi/8$, $\pi/16$, and $\pi/32$ radians are assigned to the individual elements so that the total phase shift can be any multiple of $\pi/32$ radians. The individual phase shifting elements are reflective-type devices consisting of a section of waveguide with a variable short at the end and a varactor diode mounted across the waveguide parallel to the E field of the dominant waveguide mode. The diode is operated in two different states controlled by two different bias levels applied to the diode by means of a folded choke bias connector.

The phase shifter was designed with the knowledge that it was to be controlled by the output of a digital computer having known output signals. High speed biasing circuits were developed to translate the output signals of the computer into proper biasing voltages for the diodes.

Two other microwave devices were developed in addition to the phase shifter. One was a phase detector capable of measuring the performance of the phase shifter within the desired accuracy. The other device was a phase distortionless power limiter for reducing any amplitude modulation not eliminated in the phase shifter design.

The completed phase shifter produced phase transient times of approximately 10 nanoseconds at an operating frequency of 9.370 GHz. Amplitude modulation, not including amplitude modulation occuring during transients, was limited to 1 percent. The overall accuracy of the phase shifter was approximately $\pi/64$ radians for any phase state. The insertion loss of the phase shifter-limiter combination was about 25 db.

Thesis Supervisor: J. Francis Reintjes

Title: Professor of Electrical Engineering

Acknowledgement

The research reported in this document was made possible through the use of the research facilities provided by the Electronic Systems Laboratory at M. I. T., under Contract AF-33(657)-8932, M. I. T. Project 9247.

Grateful acknowledgement is made to Mr. R. W. Roig, who originally inspired this research; to Messrs. J. O. Silvey, D. N. Brewster, and P. Ver Planck for their helpful suggestions; and to the drafting and publications staff of the Electronic Systems Laboratory for their efforts in preparing this document.

CONTENTS

CONTENTS (Cont.)

LIST OF FIGURES

LIST OF FIGURES (Cont.)

A HIGH SPEED, DIGITAL, X-BAND PHASE SHIFTER

CHAPTER I

INTRODUCTION

Certain applications of microwave signals require phase shifts of high accuracy to be added to the microwave signal. One of the best ways of accomplishing this is to add the phase shifts of a number of binary phase shifting elements.

This thesis concerns the development of a high speed digital X-band phase shifter designed to operate at power levels of less than 100 mw and over a bandwidth of less than 10KHz*. Phase shifting is accomplished by six binary phase shifting elements incorporated in microwave circuitry that adds the phase shifts of the individual elements.

Phase shifts of π, $\pi/2$, $\pi/4$, $\pi/8$, $\pi/16$, and $\pi/32$ radians are assigned to the individual elements so that the total phase shift can be any multiple of $\pi/32$ radians. The individual phase shifting elements are reflective-type devices consisting of a section of waveguide with a variable short at the end and a diode mounted across the waveguide parallel to the E field of the dominant waveguide mode. The diode is operated in two different states controlled by two different bias levels applied to the diode by means of a folded choke biasing connector.

The design objective for the phase shifter included (a) minimizing any amplitude changes that might accompany phase shifts (with a

---

* Hz (Hertz), as adopted by the National Bureau of Standards, denotes cycles per second.

constant loss being relatively unimportant), (b) obtaining transient times of 10 nanoseconds or less for a phase increment, and (c) an overall accuracy of within $\pi/64$ radians for any phase state.

The phase shifter was designed with the knowledge that it was to be controlled by the output of a digital computer having known output signals. In order to translate the output signals of the computer into the proper voltages for biasing the diodes, high speed biasing circuits had to be developed. The phase shifting system is shown schematically in Fig. 1.1.

Two other microwave devices were developed in addition to the phase shifter. One was a phase detector capable of measuring the performance of the phase shifter within the desired accuracy. The other device was a phase distortionless power limiter to be used in conjunction with the phase shifter to lessen any amplitude modulation that might not have been eliminated in the design of the individual phase shifting elements.

The resulting phase shifter produced phase transient times of approximately 10 nanoseconds at an operating frequency of 9.370GHz. Amplitude modulation, not including amplitude modulation occuring during transients, was limited to 1 percent. The overall accuracy of the phase shifter met the design objective of $\pi/64$ radians for any phase state.

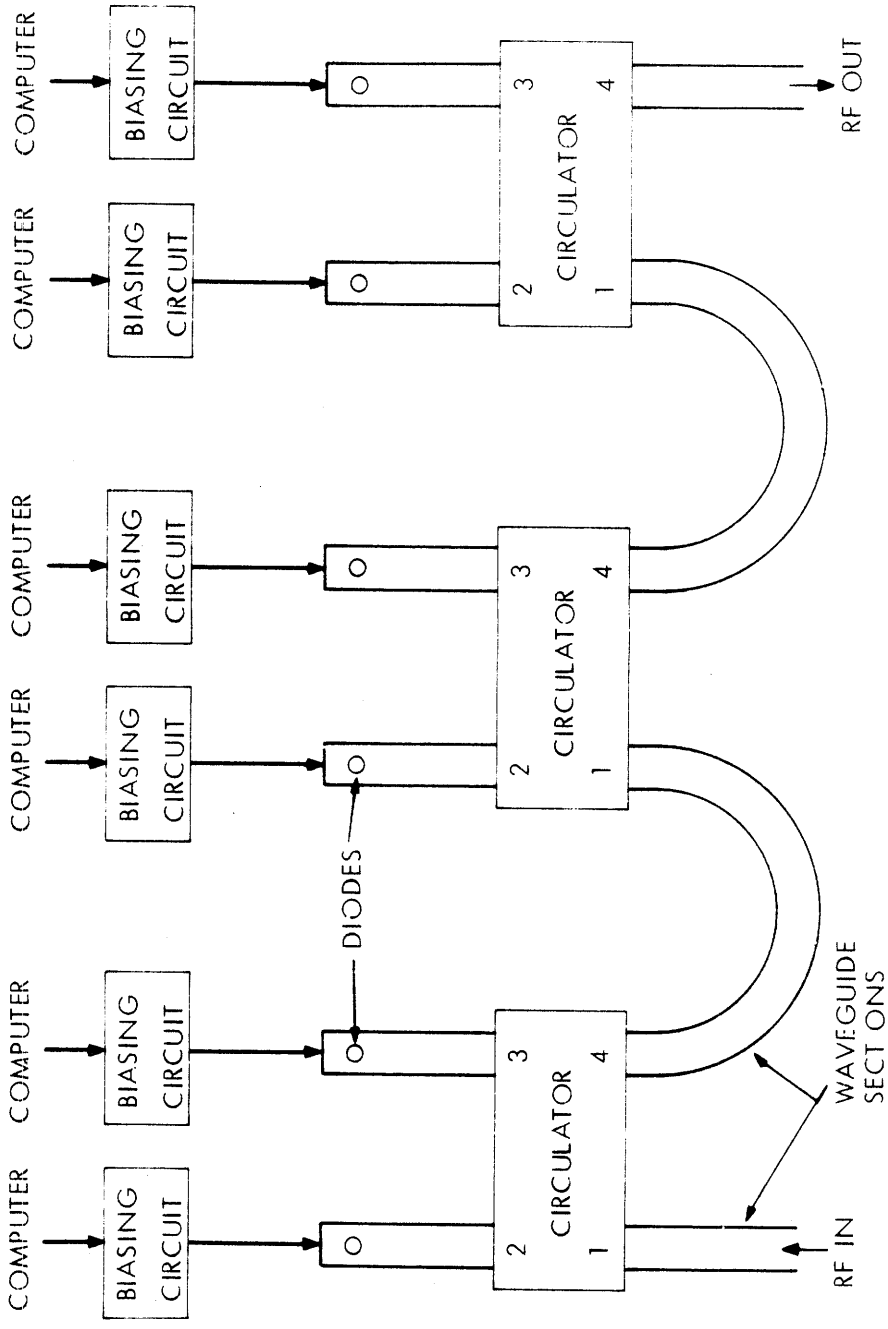

Fig. 1.1 Configuration of Phase Shifting System

CHAPTER II

ANALYSIS OF THE PHASE SHIFTING CAPABILITIES OF SEMICONDUCTOR DIODES IN A REFLECTIVE TERMINATION

2.1 Background

The use of semiconductor diodes for microwave phase shifting has been investigated by a number of people. Rutz[1] found that IN263 crystal diodes could be used for frequency, phase, or amplitude modulation. Hardin et al.[2] used varactor diodes for phase shifting, but could only get 41 degrees of phase shift with a single diode at X-band. Some theoretical calculations on the work done by Hardin were made by Searing.[3] Cohen[4] also had the problem of needing more than one diode for a 180 degree phase shift. Garver[5] found the requirements on both varactor diodes and switching diodes for achieving 180 degree phase shifts without amplitude modulation.

The investigators mentioned above used reflective-type devices that could be made into transmission-type devices through the use of 3 db couplers or circulators. Transmission-type phase shifting devices have also been investigated. Dawirs[6] and White[7] have investigated the reactive loading of a transmission line for phase shifting. Unfortunately, this method of phase shifting requires more than one diode for a 180 degree phase shift and there are inherent problems of amplitude modulation (as with the reflective-type phase shifting).

Of the two methods of phase shifting investigated, the reflective-type devices seemed more practical in view of the large number of diodes that seem to be necessary for 180 degree phase shifts with transmission-type devices. One of the important drawbacks of the reflective

phase shifting methods studies is the amplitude modulation that accompanies phase modulation. Of the investigators mentioned, Garver is the only one who found an explicit criterion for obtaining a phase shift without amplitude modulation. However, this was only done for a 180 degree phase shift. A more general solution of the problem has apparently not been found.

2.2 Diode Equivalent Circuits

The formulation of an appropriate model of a diode mounted in a waveguide section is necessary for the analysis of the phase shifting capabilities of the diode. Before this can be done, however, a model of the diode alone must be formulated.

One of the most commonly used models of a semiconductor diode is shown in Figure 2.1. L_s is the inductance produced by the physical length of the lead connecting the terminals of the diode package to the junction. C_j is the junction capacitance due to the depletion layer. The value of C_j is determined by the width and area of the depletion layer. The width of the depletion layer is a function of bias voltage which, therefore, makes C_j a function of bias voltage. R_p represents the nonlinear resistance associated with the semiconductor and is a function of bias voltage. R_s represents the spreading resistance of the semiconductor, which is assumed to be constant in this study.

With varactor diodes C_j is a relatively strong function of reverse voltage and becomes larger and larger as the magnitude of the reverse voltage is decreased. A normalized plot of C_j versus reverse voltage is shown in Figure 2.2 for a typical varactor diode. C_j varies very little with bias voltage in PIN

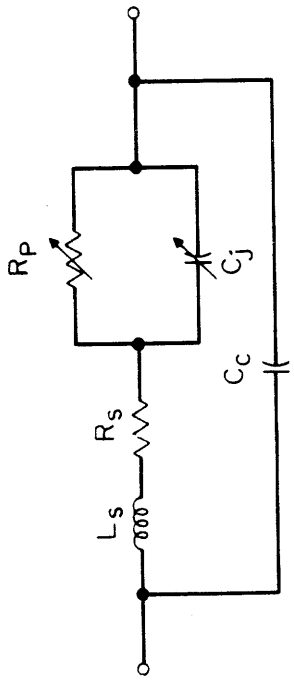

Fig. 2.1 Semiconductor Diode Model

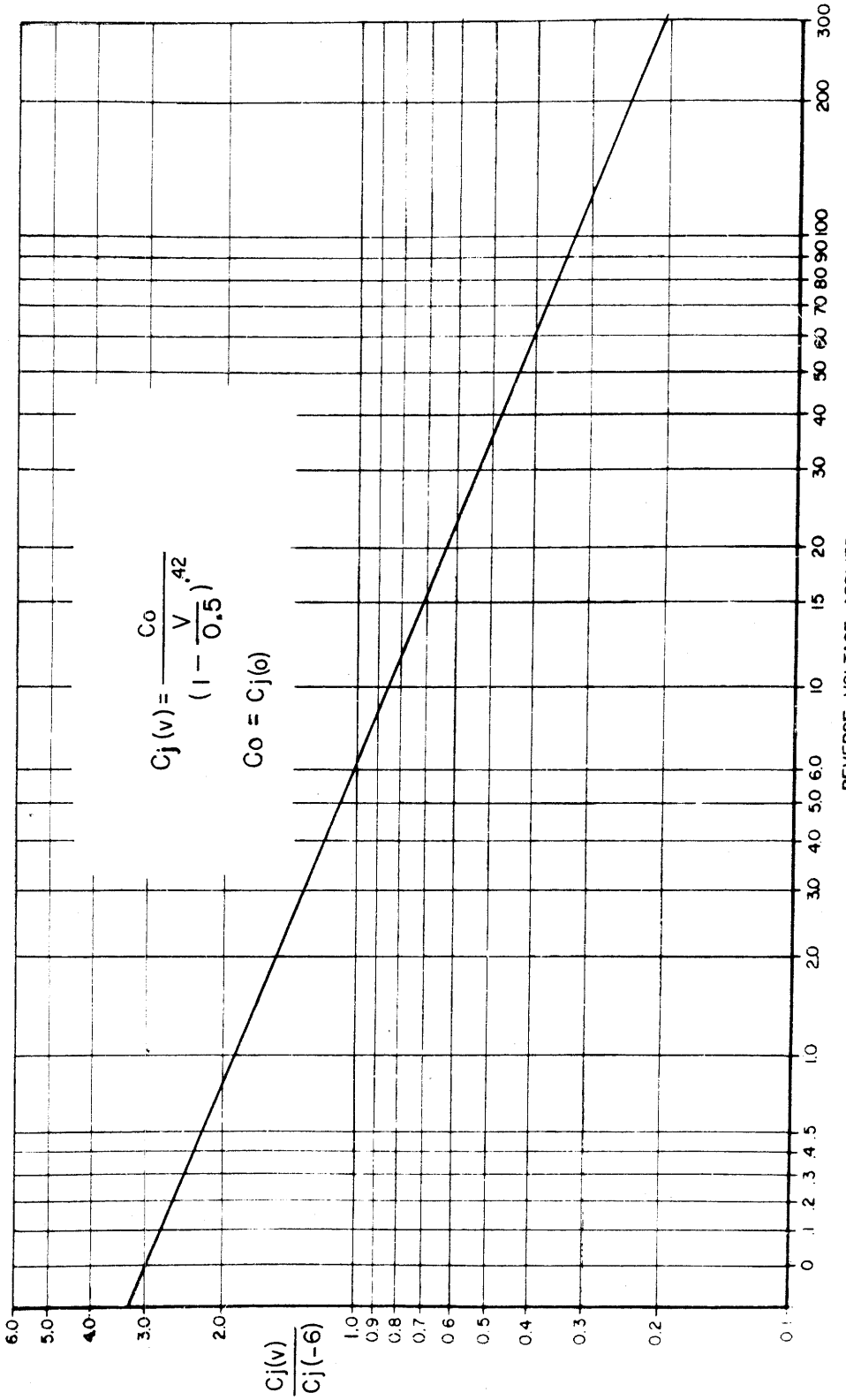

Fig. 2.2 Ratio of Junction Capacitance at Reverse Bias Voltage (-v) to Junction Capacitance at 6 Volts Reverse Bias. (Adapted From American Electronic Laboratories)

and crystal diodes. In all three types of diodes mentioned, R_p is usually large enough to be neglected with reverse bias voltages and small enough with forward bias voltages so that C_j can be neglected.

C_c includes the parasitic capacitances that arise from the semiconductor supports and the proximity of the anode to the cathode.

More exact models than the one shown in Figure 2.1 can be found from examination of the particular type of packaging a diode manufacturer might use. For example, the two basic varactor diode package styles of the American Electronic Laboratories shown in Figure 2.3 have the equivalent circuits shown in Figure 2.4. Here R_p has been omitted because it is assumed that the diodes are operating in their reverse voltage region where R_p is much larger than $\frac{1}{C_j\omega}$. The inductances are calculated from the formula for the inductance of a straight wire:[17]

$$L = .002s(\ln \frac{4s}{d} - \frac{3}{4} + \frac{d}{2s}) \qquad (2.1)$$

where L is the inductance in microhenries, s in the length of the wire in centimeters and d is the diameter in centimeters. The permeability of the wire is assumed equal to the permeability of free space. In the cartridge case the .25nH is a result of the inductance of 4 fine wires that are connected in parallel to the anode and crystal. The contact point at the crystal is the semiconductor junction. The 2.5 nH inductor comes from the inductance of the electrodes that form the external contacts. C_c is shown in parallel with the .25 nH inductor, C_j and R_s because most of the capacitance results from energy storage between the inner ends of the external electrodes. This

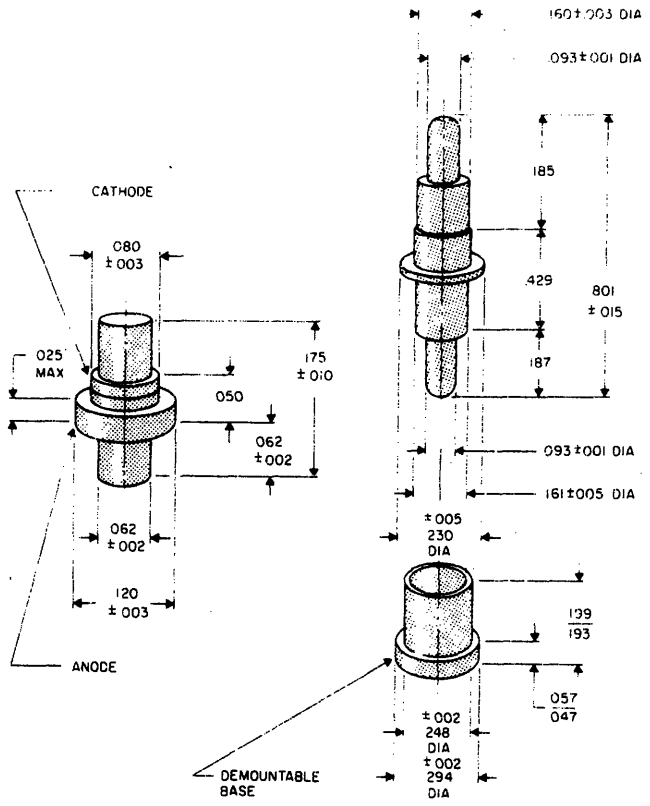

BUTTON OR PILL PACKAGE **CARTRIDGE PACKAGE**

Fig. 2.3 American Electronic Laboratories Diode Package Styles

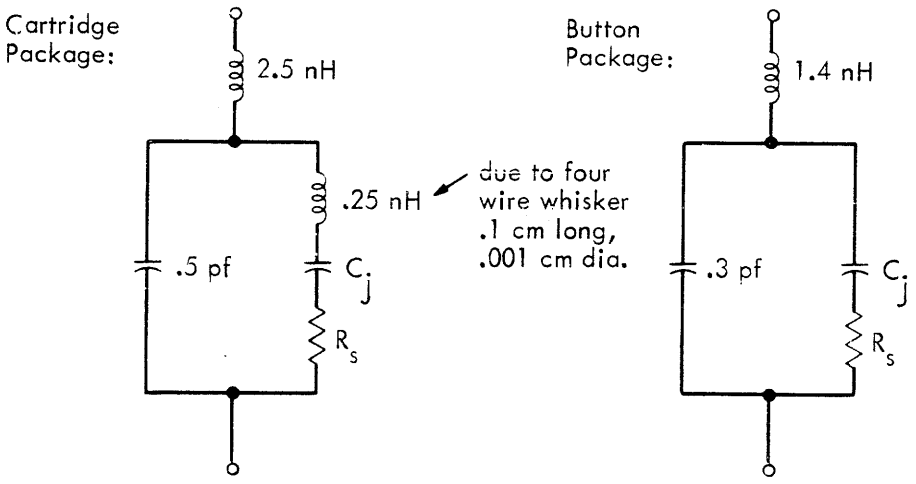

Fig. 2.4 Cartridge and Button Package Diode Equivalent Circuits

capacitance must therefore be in series with the 2.5 nH resulting from the "straight wire" inductance of these electrodes. Since the fine wires and semiconductor junction are also between the ends of the external electrodes, C_c must be put in parallel with the junction capacitance and the .25 nH inductance. The smaller size of the button package results in lower values of series inductance and case capacitance. The fine wire inductance which is in series with C_j in the cartride package model is small enough to be neglected in the button package circuit model.

2.3 Transmission Line Model

In determining the model for the interaction of the diode and rectangular waveguide, it is assumed that the diode is mounted parallel to the narrow waveguide walls and centered between them. It is also assumed that only the TE_{10} mode is propagating in the waveguide.

In general, when an obstacle is put in a waveguide it can be represented by a T-network in a transmission line as shown in Figure 2.5. Here Z_o is the characteristic impedance of the waveguide and is given by[18]

$$Z_o = \frac{2b}{a} \left(\frac{\mu}{\epsilon}\right)^{1/2} \left(1 - \frac{\lambda^2}{4a^2}\right)^{-1/2}, \qquad (2.2)$$

where b = narrow wall dimension,

a = wide wall dimension,

μ = permeability of the material inside the waveguide,

ϵ = permitivity of the material inside the waveguide,

λ = free space wavelength of the excitation.

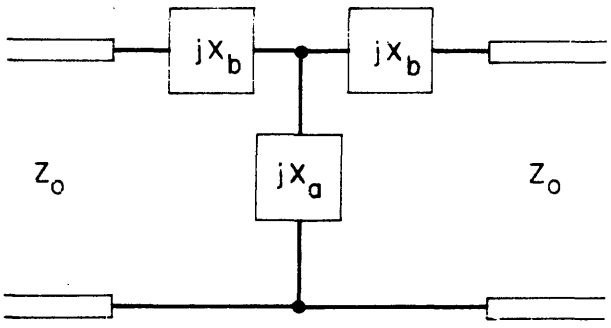

Fig. 2.5 Transmission Line Model of an Obstacle in a Waveguide

Inserting the diode in the waveguide across the E-field maximum is similar to putting a centered post of variable height in the waveguide. Marcuvitz[8] has tabulated the values of X_a and X_b for various values of the height and diameter of the post. Thick posts have relatively large values of X_b while thin posts have relatively small values of X_b. For a post 1/16 inch in diameter, X_b is about .02 Z_o at 9.370 GHz, which is nearly a short circuit. In general, X_b will be small compared to Z_o if the diameter of the post is small compared to a wavelength.

The effect of the thickness of the post on the transmission line model could have been deduced from Bartlet's Bisection Theorem applied to obstacles in waveguides.[9] Using this theorem it is easily shown that X_b goes to zero as the thickness of the obstacle goes to zero. Thus, a diode that is thin enough could be represented approximately by a single shunt element. It will henceforth be assumed that the diodes used in the phase shifter will be thin enough (compared to a wavelength) so that X_b can be neglected.

So far, nothing has been said about how the diode parameters determine X_a. Intuitively, one would guess that X_a could be replaced by the diode equivalent circuit. Fortunately, Z_o was chosen in order to obtain the correct value of power flow W from the expression

$$W = \frac{V^2}{2Z_o} , \qquad (2.3)$$

where V is defined as b times the electric field at the center of the waveguide. This choice of Z_o results in the resistance and inductance values for the transmission line model of a thin centered post in a waveguide being very similar to the values one would calculate in the

absence of the waveguide.[10] Using the diode equivalent circuit as the shunt element in the transmission line model thus appears to be the logical thing to do. It also predicts results that have experimentally been found to be approximately correct.[11]

2.4 Calculation of Phase Shifts

The transmission model to be used for the calculation of the possible phase shifts that can be produced with semiconductor diodes is shown in Figure 2.6. The impedance at z = -a as seen looking toward the right in the transmission line model is $R_s + j\left(L_s\omega - \frac{1}{C_j\omega}\right)$ in parallel with $jx = \frac{-(jZ_o\tan\beta_g a)\frac{1}{C_c\omega}}{Z_o\tan\beta_g a - \frac{1}{C_c\omega}}$, where β_g is the propagation constant in the waveguide. By varying a, jx can be made any value between $-j\infty$ and $+j\infty$. The reflection coefficient at z = -a is, therefore,

$$\Gamma(-a) = \frac{Z(-a) - Z_o}{Z(-a) + Z_o}$$

$$= \frac{x\left(\frac{1}{C_j\omega} - L_s\omega\right) - Z_oR_s - j\left[Z_o\left(L_s\omega - \frac{1}{C_j\omega}\right) + x(Z_o - R_s)\right]}{x\left(\frac{1}{C_j\omega} - L_s\omega\right) + Z_oR_s + j\left[Z_o\left(L_s\omega - \frac{1}{C_j\omega}\right) + x(Z_o + R_s)\right]} \qquad (2.4)$$

2.4.1 Varactor Diodes as Phase Shifting Elements

In the varactor diode C_j can be varied with reverse bias voltage. Thus a change in the bias voltage will cause a change in $\Gamma(-a)$ and a phase shift will result.

The behavior of the $\Gamma(-a)$ function for the varactor diode can be studied by plotting a family of curves with different C_j and

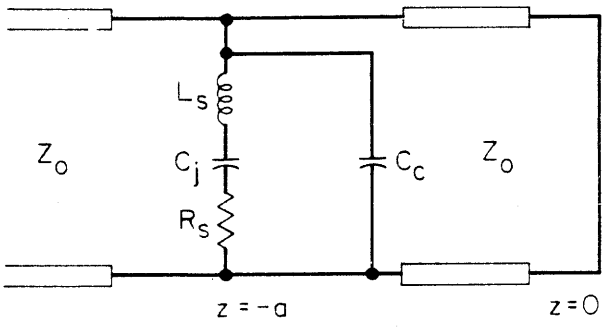

Fig. 2.6 Transmission Line Model for Phase Shift Calculation

the same ω, Z_o, R_s, and L_s versus x. Alternatively, the $\Gamma(-a)$ function can be plotted against C_j, but this type of plot is more difficult to understand physically than a plot of $\Gamma(-a)$ versus x. Figures 2.7 and 2.8 show a few of the $\Gamma(-a)$ curves with $Z_o = 500$ ohms, $f = \frac{\omega}{2\pi} = 10$ GHz, $L_s = 2.0$ nH and $R_s = 10$ ohms. These curves are most easily found from the $Z(-a)$ function and a Smith Chart. The $\Gamma(-a)$ function is shown in the region of x where significant changes occur. Phase shifts would occur when C_j was switched from one value to another at a particular x.

It can be seen from Figs. 2.7 and 2.8 that x has very little effect on $\measuredangle \Gamma^*(-a)$ for certain values of capacitance, while phase changes of over 180 degrees occur in a relatively narrow region of x for other values of capacitance. The $\measuredangle\Gamma(-a)$ passes through zero for these large phase changes. Physically what is happening when $\measuredangle \Gamma(-a) = 0$ is that a parallel resonant circuit is formed at $z = -a$ which presents a large (greater than Z_o) real impedance at this point. It would seem that this tuned condition should occur for any value of C_j. Indeed, it is easily shown that for a parallel resonance to occur, one need only choose x so that

$$x = \frac{R_s^2 + (L_s\omega - \frac{1}{C_j\omega})^2}{\frac{1}{C_j\omega} - L_s\omega} \qquad (2.5)$$

However, if $\measuredangle\Gamma(-a)$ is to be zero under this condition, the magnitude of the impedance at $z = -a$ must be greater than Z_o or

$$R_s^2 + (L_s\omega - \frac{1}{C_j\omega}) > Z_o R_s \qquad (2.6)$$

It is usually possible to have a phase change without any change.

---

* $\measuredangle \Gamma(-a)$ means the angle of $\Gamma(-a)$.

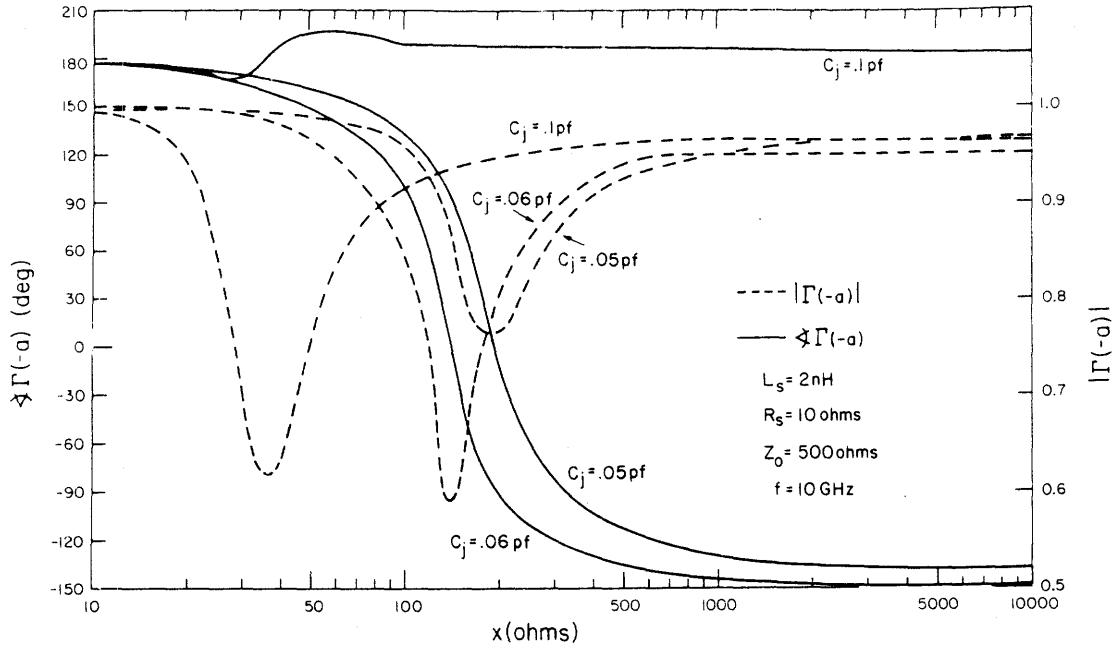

Fig. 2.7 Angle and Magnitude of Γ Curves

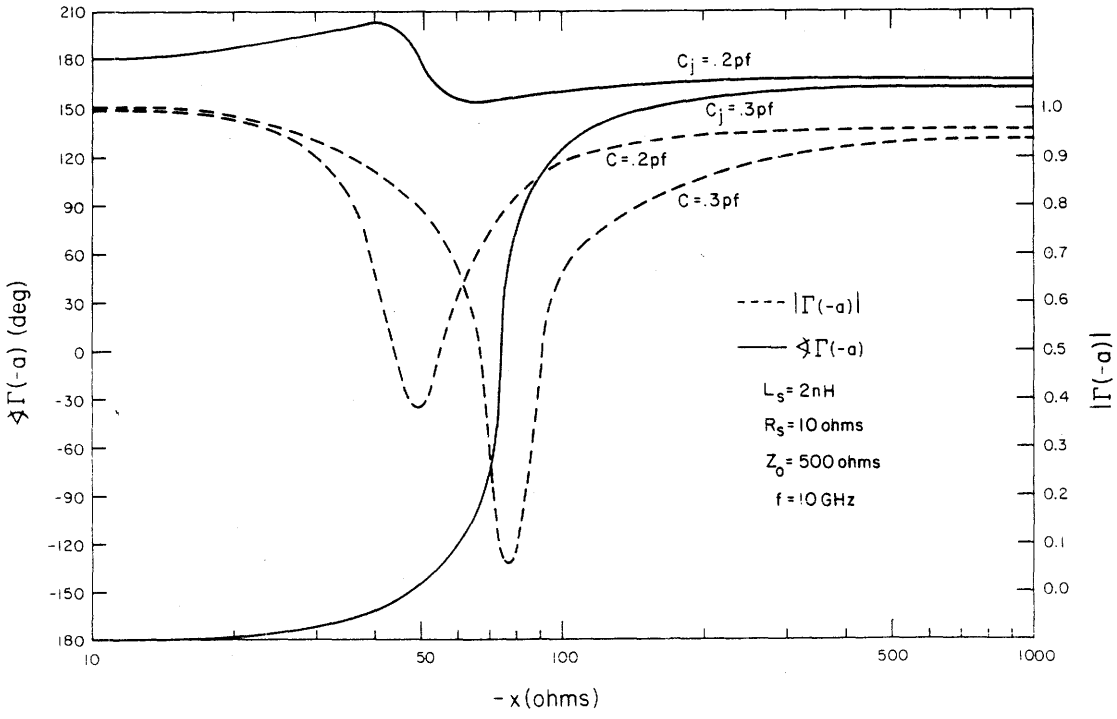

Fig. 2.8 Angle and Magnitude of Γ Curves

in $|\Gamma(-a)|$. In order for this to occur, the $|\Gamma(-a)|$ curves for the two different states of the varactor diode must intersect at the value of x at which the diode is operated. For example, Fig. 2.7 shows that a phase change of about 100 degrees will occur without any change in $|\Gamma(-a)|$ between the C_j = .06 pf and C_j = .05pf curves at $x \cong 180$ ohms. It would appear that any desired phase shift between 0 and 180 degrees could be made with constant $|\Gamma(-a)|$ if the appropriate combination of values of x and C_j were chosen.. However, the complexity of the $\Gamma(-a)$ function makes this somewhat difficult to prove.

The magnitude of $(L_s\omega - \frac{1}{C_j\omega})$ plays an important part in determining the power loss in the phase shifter. Since the larger phase shifts occur near the parallel resonance point where $|\Gamma(-a)|$ is at a minimum, determining how the diode parameters affect the value of $|\Gamma(-a)|$ at parallel resonance will show how the loss in the phase shifter can be minimized by choosing the diode parameters properly. At parallel resonance, $|\Gamma(-a)| = \Gamma_o$ and

$$\Gamma_o = \frac{R_s^2 + (L_s\omega - \frac{1}{C_j\omega})^2 - Z_o R_s}{R_s^2 + (L_s\omega - \frac{1}{C_j\omega})^2 + Z_o R_s} \quad . \tag{2.7}$$

It is easily seen that Γ_o can be maximized by minimizing $Z_o R_s$ and maximizing $(L_s\omega - \frac{1}{C_j\omega})^2$. A high cutoff frequency, $f_c = \frac{1}{2\pi R_s C_j}$, is necessary for a small R_s. Eq. 2.2 shows that Z_o can be reduced by using a reduced height waveguide. In order to maximize $(L_s\omega - \frac{1}{C_j\omega})^2$ and yet allow C_j to vary this quantity significantly, it

is necessary to use a low-capacitance diode, preferably with a high-breakdown voltage. The high breakdown voltage allows for a large variation of C_j. The use of a pill or button package would also help to maximize $(L_s\omega - \frac{1}{C_j\omega})$ since L_s is relatively small for this type of package.

2.4.2. PIN Diodes as Phase Shifting Elements

In the PIN diode, C_j does not vary appreciably with reverse voltage. A forward bias is necessary to change $\Gamma(-a)$ significantly. Under forward bias conditions R_p becomes small enough so that C_j can be neglected. The value of R_p ranges typically from thousands of ohms at zero bias to a fraction of an ohm with tens of milliamperes bias current. The $\Gamma(-a)$ function derived previously holds for the PIN diode in a forward bias condition if $\frac{1}{C_j\omega}$ is replaced by zero and the variation of R_p is included in R_s.

As with a varactor diode, the phase shift available with a PIN diode can be found by taking the difference between $\measuredangle \Gamma(-a)$ for the two bias states. When the PIN diode is forward biased, the equivalent transmission line circuit at $z = -a$ is a series RL circuit in parallel with jx. When the diode is reverse biased, a series RLC circuit in parallel with jx is formed. If C_j is considered as the only parameter affected by bias, then there are only two $\Gamma(-a)$ curves for the diode, one for forward bias and one for reverse bias. However, R_s can be used as a parameter for generating more $\Gamma(-a)$ functions with different forward bias current levels. A condition for achieving significant phase shifts is that $\measuredangle \Gamma(-a)$ versus x must pass through zero and that the point at which it passes through zero must

depend on the parameters regulated by bias level. Eq. 2.5 shows that this point does depend on R_s. Thus, a family of $\Gamma(-a)$ versus x curves with R_s as the variable parameter can be generated, and, as with the varactor diodes, phase shifts can conceivably be made with no amplitude modulation at the points where the $|\Gamma(-a)|$ curves intersect.

2.5 Diode Switching Speeds

One of the properties of the PIN diode is that it does not rectify the applied RF signal. This requires a relatively long minority carrier lifetime which tends to conflict with the requirement of a fast switching speed (if the diode were operated between forward and reverse states), since the minority carrier lifetime determines how long it takes for the diode to go from a reverse bias state to a forward bias state.[12]

The varactor diode does not need to be switched between forward and reverse bias states to produce a phase shift. The limitation on the switching speed is determined mainly by the time constant associated with the diode circuit model. If the diode is mounted in such a way that L_s is negligible, the time constant for R_s = 10 ohms and C_j = .2pf is $R_s C_j = 2 \times 10^{-12}$ seconds. Thus, this type of limitation causes no conflict with the design objective of a phase shift transient time of less than 10 nanoseconds. Unlike the PIN diode, which requires a bias current of 40 to 50 milliamperes in the forward bias state to make the series resistance tolerably small, the varactor diode draws currents on the order of a microampere in its operating states. These low current levels are somewhat easier to switch rapidly than the PIN bias currents.

Thus, if the PIN diode were operated only in the forward bias state and phase shifts were achieved by switching between different values of R_s, rapid switching would still be difficult even though the minority carrier lifetime played no part in the switching process.

Because of the apparently greater ease with which varactor diodes can be switched rapidly, it was decided that these diodes would be used instead of PIN diodes in the phase shifting system.

CHAPTER III

THE PHASE DETECTOR

A fast, accurate phase detector was necessary to measure the performance of the phase shifting system. The phase detector had to be fast enough to accurately measure the rise and fall times of the step phase shifts produced by the phase shifter and accurate enough to measure the smallest phase increment ($\pi/32$) produced by the phase shifter.

The method of phase detection that was used is based on a modification of the principle of "An Automatic Microwave Phase Comparator".[13] The modification was made so that the phase detector would be relatively insensitive to changes in the amplitude of the detected microwave signal.

3.1 Theory

If the two signals containing the phase difference that we wish to detect are $Ae^{j\phi/2}$ and $Be^{-j\phi/2}$, the sum and difference of these signals can be formed with the appropriate microwave circuit to give

$$E_a = Ae^{j\phi/2} - Be^{-j\phi/2} \qquad (3.1)$$

and

$$E_b = Ae^{j\phi/2} + Be^{-j\phi/2}. \qquad (3.2)$$

If the amplitudes of these signals are detected by linear microwave amplitude detectors, we get

$$E_{ad} = K \quad (A^2 + B^2 - 2AB \cos \phi)^{\frac{1}{2}} + C \qquad (3.3)$$

and

$$E_{bd} = K \quad (A^2 + B^2 + 2\,AB \cos \phi)^{\frac{1}{2}} + C\,. \qquad (3.4)$$

In Eqs. 3.3 and 3.4 it has been assumed that the parameters of the detectors, K and C, are the same for both detectors.

We can eliminate the effect of amplitude changes of one of the signals by making it much larger than the amplitude of the other signal. If A is varying in amplitude, we make A much greater than B. Then, E_{ad} and E_{bd} reduce to

$$E_{ad} = KA \quad (1 + \frac{B^2}{A^2} - \frac{2B}{A} \cos \phi)^{\frac{1}{2}} \cong KA\,(1 - \frac{B}{A} \cos \phi) + C \qquad (3.5)$$

and

$$E_{bd} = KA \quad (1 + \frac{B^2}{A^2} + \frac{2B}{A} \cos \phi)^{\frac{1}{2}} \cong KA\,(1 + \frac{B}{A} \cos \phi) + C. \qquad (3.6)$$

The difference of the two signals can be formed with an appropriate network to give

$$E_{bd} - E_{ad} = 2KB \cos \phi\,. \qquad (3.7)$$

Thus, we have a signal that is independent of A and varies only with ϕ.

If a 90 degree phase lag is added to $Ae^{j\phi/2}$, we get

$$E_a' = Ae^{j(\frac{\phi}{2} - \frac{\pi}{2})} - Be^{-j\frac{\phi}{2}} \qquad (3.8)$$

and

$$E_b' = Ae^{j(\frac{\phi}{2} - \frac{\pi}{2})} + Be^{-j\frac{\phi}{2}}\,. \qquad (3.9)$$

Then,

$$E'_{ad} = K (A^2 + B^2 + 2AB \sin \phi)^{\frac{1}{2}} + C \qquad (3.10)$$

and

$$E'_{bd} = K (A^2 + B^2 - 2AB \sin \phi)^{\frac{1}{2}} + C . \qquad (3.11)$$

Making A much greater than B gives

$$E'_{ad} \cong KA (1 + \frac{B}{A} \sin \phi) + C \qquad (3.12)$$

and

$$E'_{bd} \cong KA (1 - \frac{B}{A} \sin \phi) + C . \qquad (3.13)$$

Therefore,

$$E'_{ad} - E'_{bd} = 2 KB \sin \phi . \qquad (3.14)$$

If $E'_{ad} - E'_{bd}$ is put on the y-axis of an oscilloscope and $E_{bd} - E_{ad}$ is put on the x-axis, a polar coordinate plot will result on the oscilloscope screen to give ϕ as the angle between the radius vector and x-axis.

3.2 Implementation of the Theory

The phase detector that was constructed with the theory of Sec. 3.1 in mind is shown schematically in Fig. 3.1. The microwave circuit consists of two magic tees, one H plane tee, a 90 degree hybrid coupler, four tunable detector mounts and two matched loads.

The input signal with the varying amplitude, $Ae^{j \phi/2}$, is fed into the H arm of the H plane tee. The reference signal with the constant amplitude, $Be^{-j \phi/2}$, is fed into one port of the 90 degree coupler, as shown in Fig. 3.1. In the upper magic tee, the two signals are added and

subtracted in the H and E plane arms and fed into tunable detectors. The 90 degree hybrid adds a phase lag of 90 degrees to the reference signal that is fed into the lower magic tee.

1N23E crystals are used as the detecting elements in the four tunable detectors. Although these crystals are commonly used as square low detectors, they provide relatively good linear detection at power levels of 10 milliwatts and over. A typical response curve for a 1N23E crystal is shown in Fig. 3.2.

The outputs of each pair of crystals is fed into an adding circuit. In order for the adding circuits to perform the functions given in Eq. 3.7 and 3.14, one of the crystals in each pair must be reversed in its mount. The adding circuitry is shown in Fig. 3.3. The 200 ohm potentiometer allows the "K" parameters of the crystal detectors (in Eqs. 3.3 and 3.4) to be matched, while the 100 ohm potentiometer equalizes the "C" parameters.

3.3 Accuracy

The accuracy of the phase detector was tested with the measuring set-up shown in Fig. 3.4. For this measurement the phase detector was adjusted so that variations of up to 10 percent in the signal amplitude would not affect the phase detector output. This was accomplished by putting a matched load at the reference signal input port of the 90° hybrid coupler and adjusting the "C" and "K" parameters of the crystal detectors so that $E_{bd} - E_{ad}$ and $E'_{ad} - E'_{bd}$ were zero (see Eqs. 3.7 and 3.14) independent of a 10 percent amplitude modulation in the input signal.

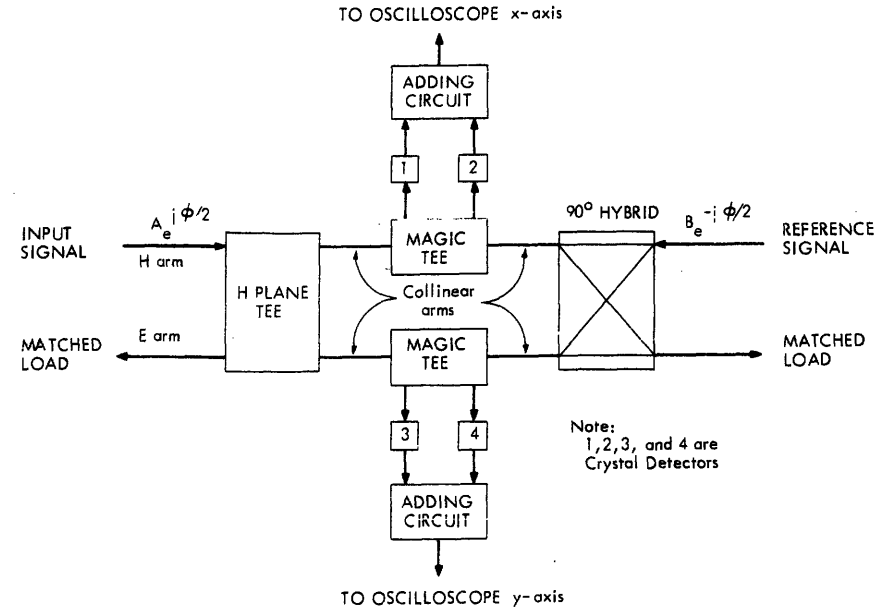

Fig. 3.1 PHASE DETECTOR

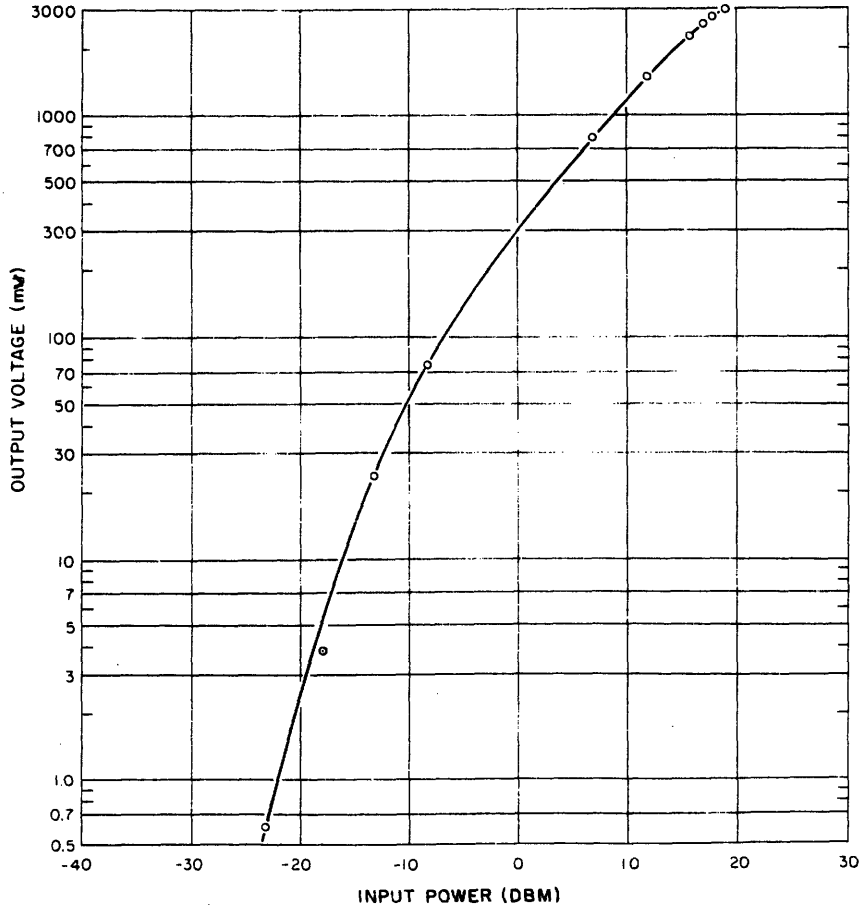

Fig. 3.2 IN23E RESPONSE IN MOUNT TUNED TO 9.370 GHz, 220 OHM LOAD

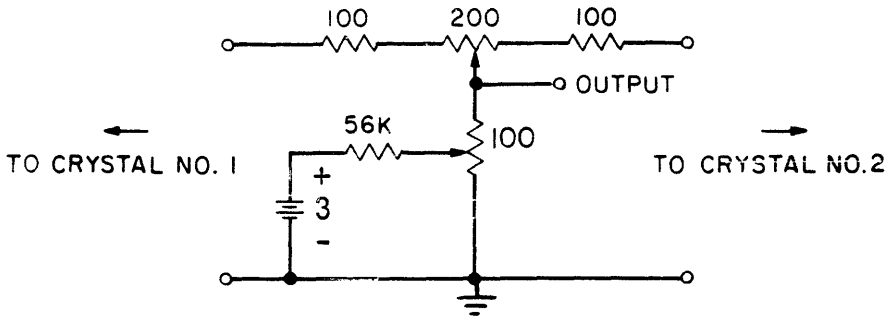

Fig. 3.3 Adding and Equalizing Circuit

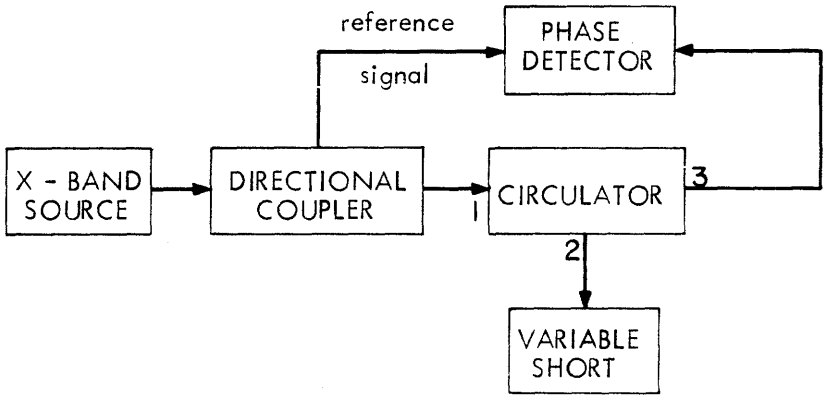

Fig.3.4 Method of Measuring Phase Detector Accuracy

The accuracy was tested by moving the sliding short through fractions of a half wavelength and noting the position of the point on the oscilloscope screen. A maximum error of 5 degrees in the position of the point was measured. However, it was found that the accuracy of the phase measurement could be greatly improved by averaging the output over the four quadrants in the oscilloscope polar plot. This was due to the error in the phase detector output being caused by a slight ellipticity in the polar phase plot. Positive errors were added in half of the plot while equal negative errors were added in the remaining half of the plot. By adding 90 degree phase shifts to the reference signal, a phase measurement could be made in each of the four quadrants of the polar plot. Phase measurements made in this manner were found to be within about 1 degree of the correct value.

CHAPTER IV

POWER LIMITING

4.1 Diodes as Power Limiters

The feasibility of using a power limiter with the phase shifter was investigated because initially it was not known whether the variations in amplitude of the phase shifted signal could be made small enough to meet the design objectives.

It is well known that the nonlinear properties of diodes can be used for low level, microwave power limiting.[14,15] With this type of limiting, the impedance presented to the RF wave in the waveguide by the diode is a function of the applied RF power. Unfortunately, most of these power limiting schemes will produce phase shifts in addition to power limiting. Any limiter that is used in conjunction with the phase shifting system must have negligible phase shifts in its power limiting region, unless it is only used to limit amplitude modulation in the transient times between phase states.

4.2 Requirements for Phase Distortionless Power Limiting

Let us suppose that the diode is mounted in a reflective termination so that the transmission line model for the situation is as shown in Fig. 4.1. Here, R and jX are functions of both the diode parameters and the tuning elements used in conjunction with the diode. Let us further assume that R depends on the incident power level and that

jX does not. The reflection coefficient at z = 0 is

$$\Gamma(0) = \frac{Z(0) - Z_o}{Z(0) + Z_o}$$

$$= \frac{R - Z_o + jX}{R + Z_o + jX}.$$

The angle of the reflection coefficient is

$$\measuredangle\ \Gamma(0) = \tan^{-1}\left(\frac{X}{R - Z_o}\right) - \tan^{-1}\left(\frac{X}{R + Z_o}\right).$$

If the limiter is to be phase distortionless, $\measuredangle\ \Gamma(0)$ must be a constant, independent of variations of R. This will occur only if X = 0 or X = ∞. Clearly, X = 0 is the desired solution, since X = ∞ would make $|\Gamma(0)| = 1$ independent of R. Thus, we see that it is necessary to tune out the reactive part of the diode and its mount to make the limiter phase distortionless.

The resistance, R, is a function of the component of resistance of the diode that arises when the RF signal forward biases the diode for a fraction of an RF cycle. The nonlinear resistance that arises from forward bias conditions is R_p of Fig. 2.1. With cyclic forward bias conditions, the resistance to be used in the diode model would be an average value of R_p. As the RF power level increases, the fraction of a cycle that the diode is forward biased approaches 1/2 (since the RF signal has to overcome the contact potential before forward conduction begins) and the forward conduction current increases causing R_p to become smaller. If R at low power levels is greater than Z_o, the reflection coefficient will decrease with power (assuming

the diode mount is tuned so that R goes to zero as R_p goes to zero) resulting in a limiting action with no phase distortion.

Since power limiting does not occur until the RF voltage swing exceeds the contact potential causing the diode to go into forward conduction, the limiting region of the diode can be changed by applying a D.C. bias. A D.C. back bias would thus cause the diode limiting region to occur at a higher power level since a larger RFvoltage swing would be necessary to drive the diode into forward conduction.

4.3 Experimental Results

A power limiter employing a 1N23E diode mounted in a tunable crystal mount was constructed. The tunable mount consisted of a variable shorting plane positioned behind the diode and two tuning screws in front of the diode. The positions of the short and one of the tuning screws were adjusted until a limiting action occured that was accompanied by phase shifts of less than 3 degrees throughout the limiting region.

At first the limiter was tested with the diode D.C. bias terminals short circuited. The limiting characteristics for this condition are shown in Fig. 4.2. The limiter was also tried with various bias voltages. It was found that increasing the reverse bias levels moved the limiting regions out to higher power levels, thus confirming the prediction of Section 4.2. The power limiting curve for a 1 volt reverse bias is shown in Fig. 4.3.

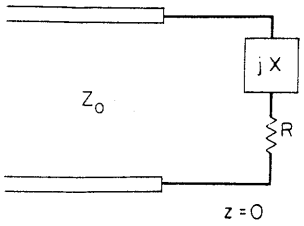

Fig. 4.1 TRANSMISSION LINE MODEL OF DIODE MOUNTED IN WAVEGUIDE FOR LIMITING

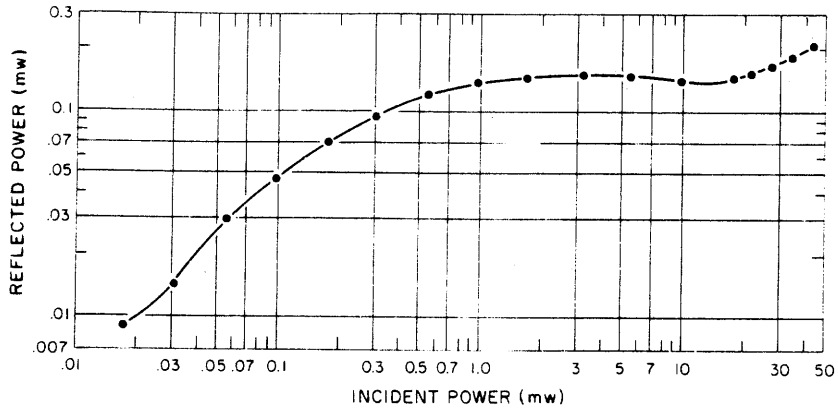

Fig. 4.2 LIMITER CHARACTERISTICS WITH BIAS TERMINALS SHORTED

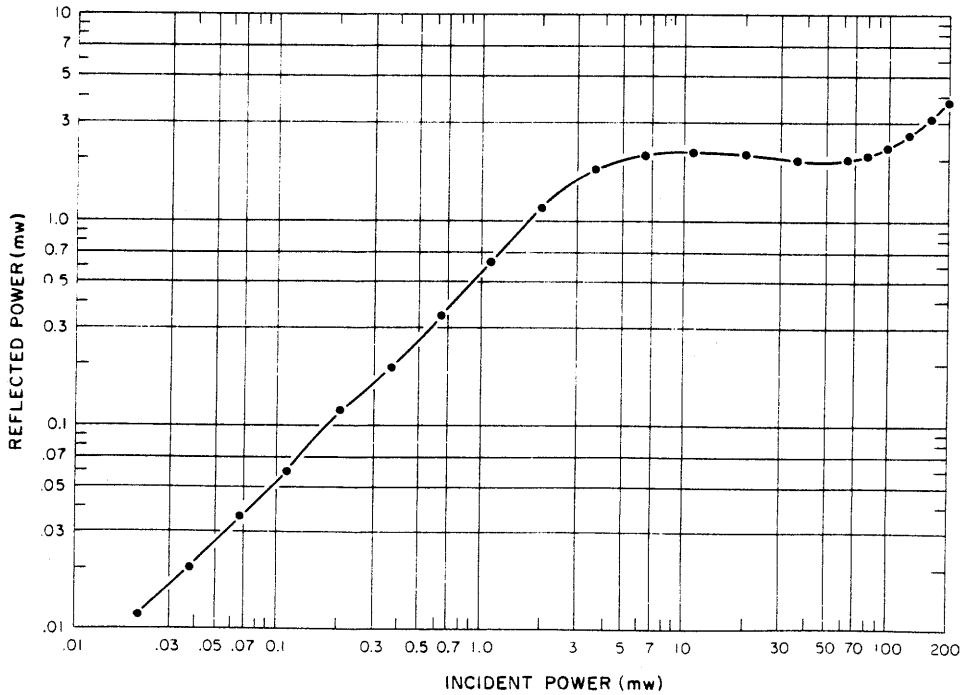

Fig. 4.3 LIMITER CHARACTERISTICS WITH 1 VOLT BACK BIAS ON DIODE

CHAPTER V

VARACTOR DIODE BIASING CIRCUITS

In order to translate the voltages levels at the output of the computer logic circuits into the voltage levels required for biasing the varactor diodes, high-speed transistor switching circuits were constructed.

5.1 Limitations of Simple Switching Circuits

The simple switching circuits shown in Figs. 5.1 and 5.2 both have one basic disadvantage: the collector to emitter capacitance must be charged through R_1 when the transistors turn off. This means that relatively low resistance values must be used if fast rise times are to be achieved. For example, a typical value of collector to emitter capacitance might be 10 pf. If we allow three RC time constants for a rise time of 10 nanoseconds, we find R_1 to be $R_1 = \frac{10^{-8}}{3 \times 10^{-11}} = 333$ ohms. Thus, if a 40 volt swing in voltage is desired, R_1 will have to be capable of dissipating $\frac{40^2}{333} \cong 5$ watts and the transistor will have to be capable of carrying a collector current of 120 ma. When a capacative load is connected to the circuits, R_1 will have to be even smaller resulting in a larger collector current. These relatively high collector currents combined with the high speed requirement put unnecessary demands on the transistors.

5.2 Complementary Four-Transistor Switching Circuit

A circuit that eliminates the problem discussed above is the complementary four-transistor switching (flip-flop) circuit. A basic model is shown in Fig. 5.3. This type of circuit replaces the

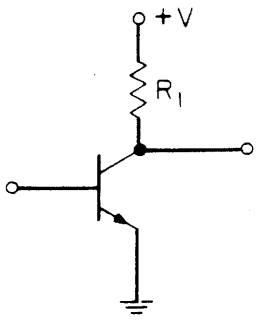

Fig. 5.1 Simple Single Transistor Switch

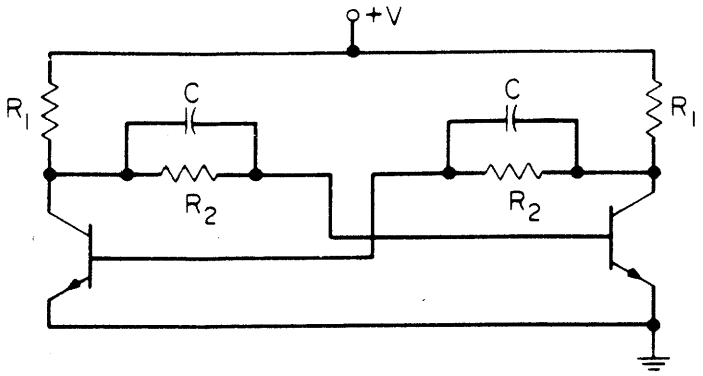

Fig. 5.2 Basic Two Transistor Switch

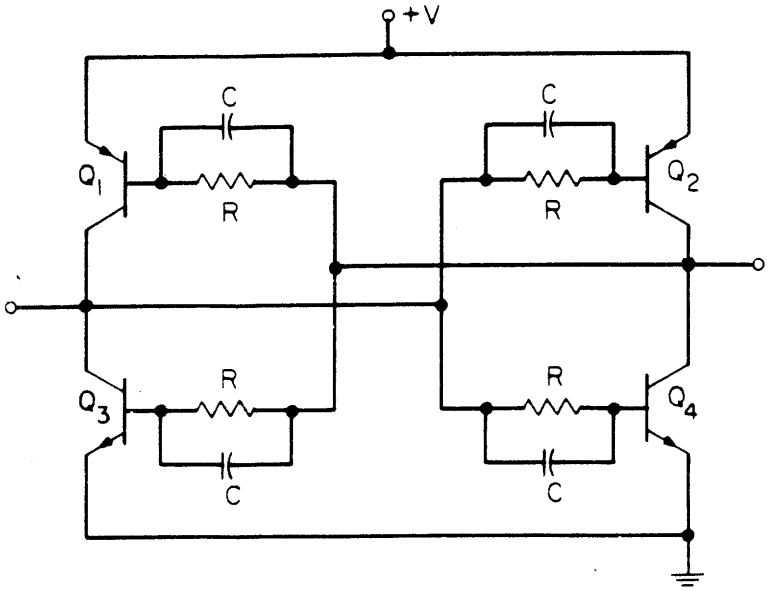

Fig.5.3 Basic Four Transistor Switching Circuit

collector resistors with transistors which are either short circuits or open circuits. Q_1 and Q_4 are either on or off together as are Q_2 and Q_3, but Q_2 and Q_3 are always in the opposite state of Q_1 and Q_4. Thus, when Q_4 turns off, its collector to emitter junction can be charged through Q_2 which is on. The problem of the RC time constant for the collector is therefore eliminated. In addition, the effect of capacitive loading on the rise time is greatly lessened.

5.3 Experimental Results

Two types of complementary four-transistor switching circuits were constructed. Both types of circuits were designed to operate in the set-reset mode by adding appropriate circuitry to the bases of the Q_3 and Q_4 transistors.

One type of switching circuit was designed to produce steps of 12 volts or less for biasing the varactor diodes producing the four smallest phase shifts. The circuit is shown in Fig. 5.4. The diodes across the base to emitter junctions were added to prevent the bias voltage from appearing across these junctions during a switching transient. Two transistors operating as simple saturated switches were added to the input circuitry to amplify the available 1 volt steps at the output of the computer logic circuitry. These transistors produce a positive going pulse with a fast rise time (about 10 nanoseconds) which is needed to trigger the flip-flop. It should be pointed out that this relatively fast rise time produced in the simple switching circuits does not contradict the discussion in Sec. 5.1, since the fast rise time is produced when the transistor turns on, not off. A fall time of about 30 nanoseconds is produced when the transistor

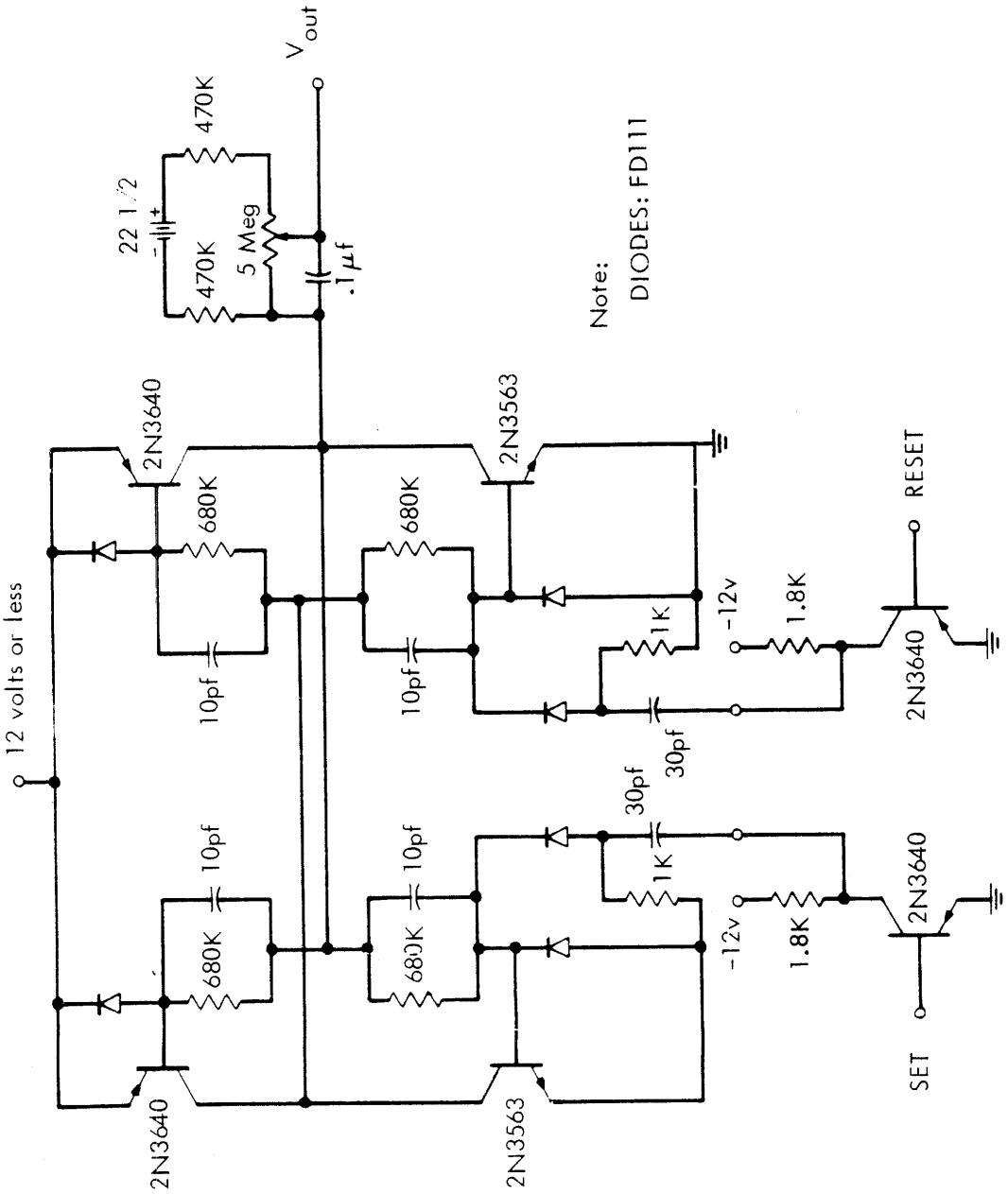

Fig. 5.4 12 Volt Switching Circuit

turns off. The circuitry at the collector output of the flip-flop enables a variable D.C. voltage to be added in series with the flip-flop output without increasing the load capacitance significantly. Rise and fall times of about 5 nanoseconds for 12 volt steps at a square wave output frequency of 5 MHz were measured at the output terminals of the flip-flop with a probe having a capacitance of 7 pf.

The other type of switching circuit is similar to one described above, except that it was designed to produce 40 volt steps or less for biasing the varactor diodes producing the two largest phase increments. This was accomplished by replacing the 2N3640 transistors with 2N2905A transistors and increasing the 680 K base resistors to 2.7 Meg. and the 10 pf speed-up capacitors to 30 pf. Rise and fall times were measured to be about 10 nanoseconds for 40 volt steps at a square wave output frequency of 1 MHz.

It was observed that capacitive loading of these circuits produced relatively little effect on the rise and fall times. However, the transistors tended to heat up in proportion to the increased capacitance because of the larger currents required to charge the capacitive load. This heating was not noticeable until the rms collector current approached the maximum current rating of the transistors and did not occur for any of the frequencies and capacitances used in the phase shifter.

CHAPTER VI

CONSTRUCTION OF THE PHASE SHIFTING ELEMENTS

6.1 Diode Selection

It was decided that a diode with a pill or button case should be used since the series inductance of this diode could be kept at a minimum by mounting the diode in a reduced height waveguide. American Electronic Laboratories varactor diodes were selected for use in the phase shifting elements. The package structure and equivalent circuit for these diodes are shown in Figures 2.3 and 2.4 respectively. The inductance shown in the equivalent circuit of the diode arises mainly from the physical length of the external leads. Thus, if the diode is mounted in a reduced height waveguide, the external leads can be buried in the waveguide walls making the effect of the inductance negligible.

6.2 Mounting the Diodes

Quarter-wave transformers were used to reduce the height of the waveguide from 0.400 inch (RG-52/U waveguide) to 0.050 inch. The transformers were designed to operate at a center frequency of 9.370 GHz. A set of tables[16] was used to aid in the design. The dimensions of the transformer steps are given in Figure 6.1. The transformer steps were made symmetrical so that a regular RG-52/U waveguide short could be used instead of one that would have to be specially designed for the reduced height waveguide. In order to facilitate soldering of the steps to the waveguide sections, they were made slightly wider than the normal RG-52/U width. Bandwidths of approximately 2 GHz

with a maximum VSWR of 1.2 were measured on the completed transformers.

In order to apply bias voltages to the diodes, folded choke biasing connectors were designed. The choke configuration is shown in Figure 6.2. A complete phase shifting element is shown in Figure 6.3.

6.3 Measured Characteristics of the Phase Shifting Elements

Curves of the magnitude and angle of the reflection coefficient at the location of the diode versus the relative position of the variable short (as read on the micrometer dial of the short) with the diode bias voltage, V_D, as a parameter were experimentally determined for the six phase shifting elements. These curves, along with the diode characteristics, are given in Figures 6.4 to 6.9. The phase detector described in Chapter III was used in determining the phase curves.

It can be seen that these curves follow qualitatively the predicted behavior reported in Chapter II. That is, $|\Gamma(-a)|$ is at a minimum when the rate of change of $\sphericalangle\Gamma(-a)$ is at a maximum which occurs under parallel resonance conditions. However, the minimum value of $|\Gamma(-a)|$, Γ_o, is considerably lower than the value predicted by Eq. 2.7. For example, the diode in phase shifting element no. 1 has a junction capacitance of approximately .13 pf at a bias voltage of -40 volts. R_s for this diode is about 4 ohms. These figures combined with a reduced height waveguide impedance of 58 ohms give $\Gamma_o \tilde{=} .97$. The measured value of Γ_o was .75. This increased loss is probably due to losses in the short and in the walls of the waveguide between the short and the diode where large circulating currents exist due to the parallel

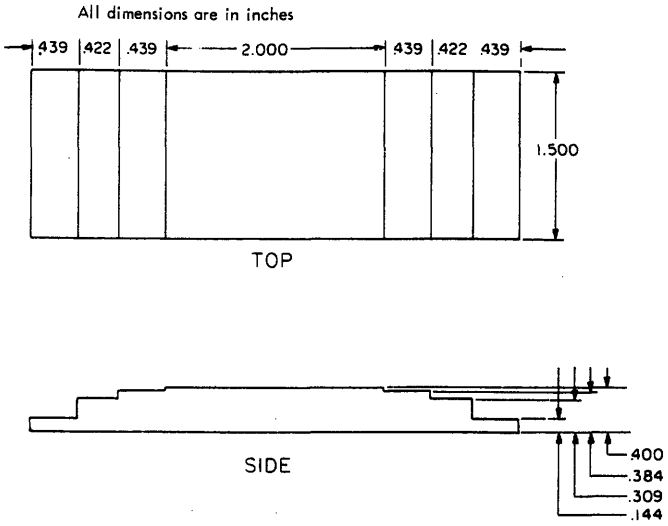

Fig. 6.1 QUARTER-WAVE TRANSFORMER STEPS

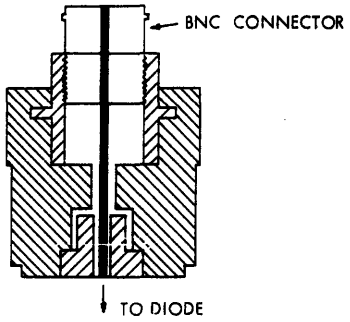

Fig. 6.2 CROSS-SECTIONAL VIEW OF FOLDED CHOKE BIAS CONNECTOR (enlarged)

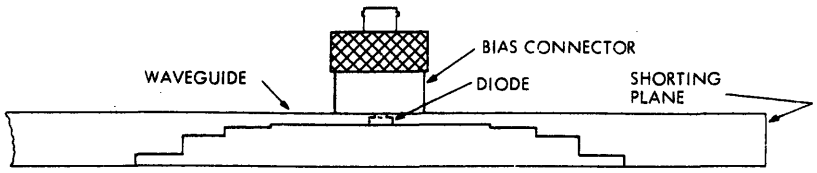

Fig. 6.3 SIDE VIEW OF COMPLETE PHASE SHIFTING ELEMENT

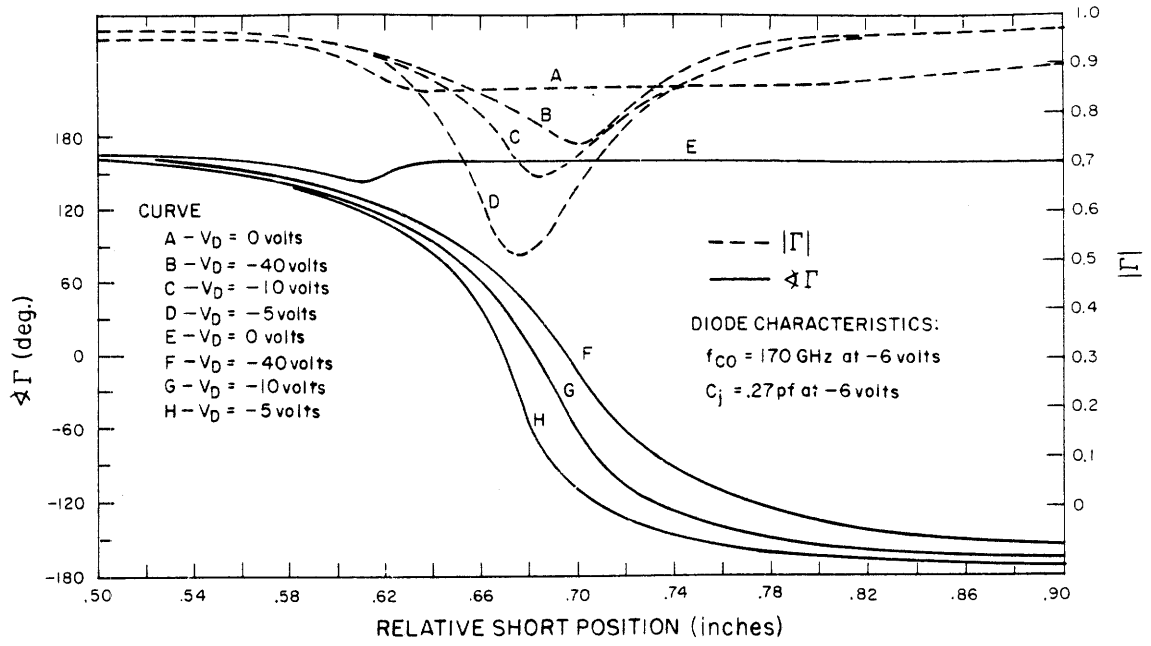

Fig. 6.4 Phase and Magnitude Characteristics of Phase Shifting Element No. 1

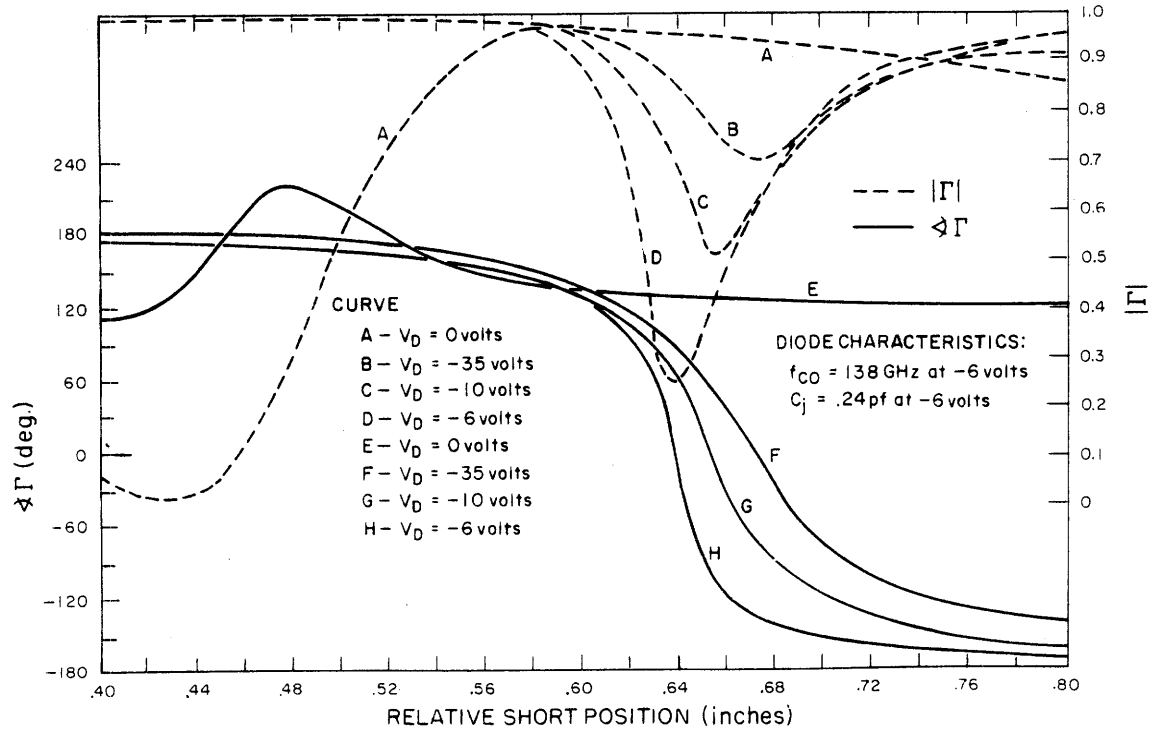

Fig. 6.5 Phase and Magnitude Characteristics of Phase Shifting Element No. 2

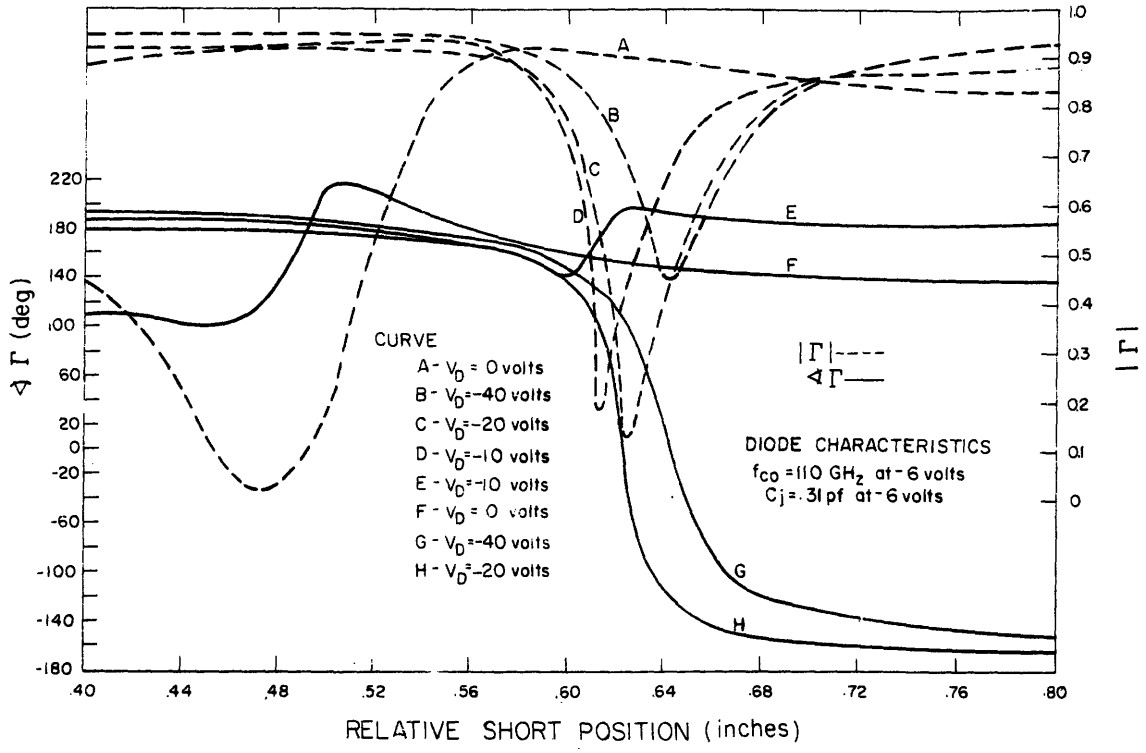

Fig. 6.6 Phase and Magnitude Characteristics of Phase Shifting Element No. 3

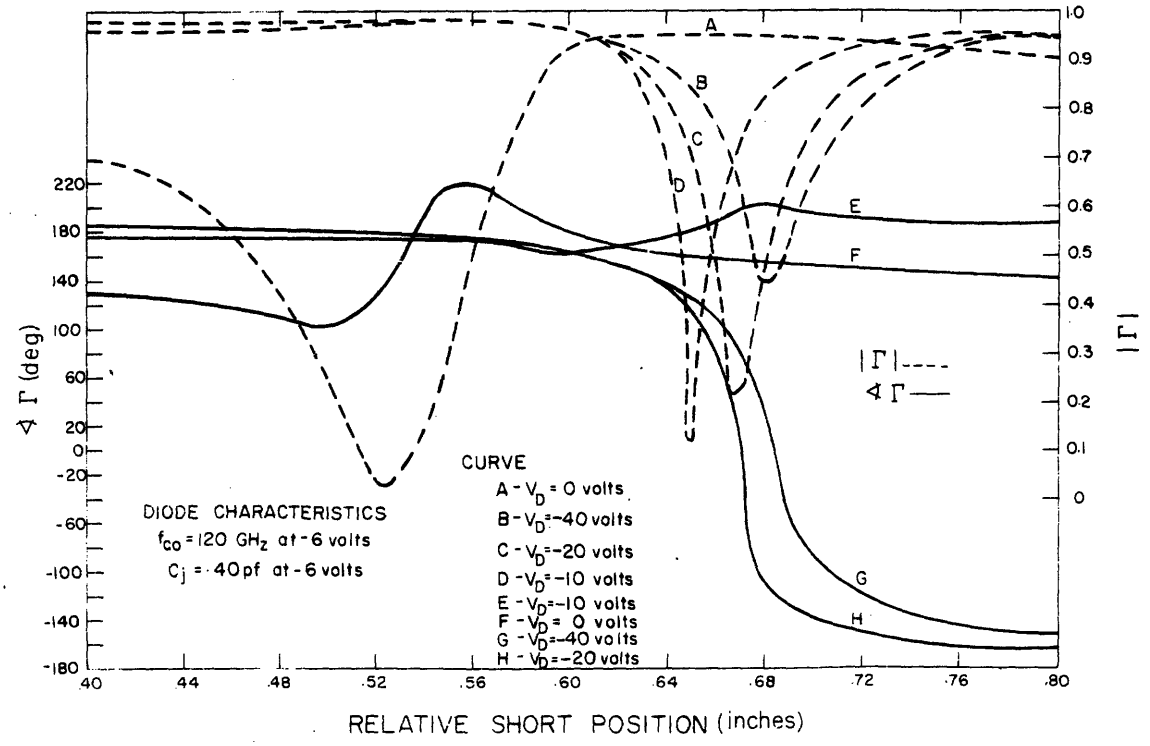

Fig. 6.7 Phase and Magnitude Characteristics of Phase Shifting Element No. 4

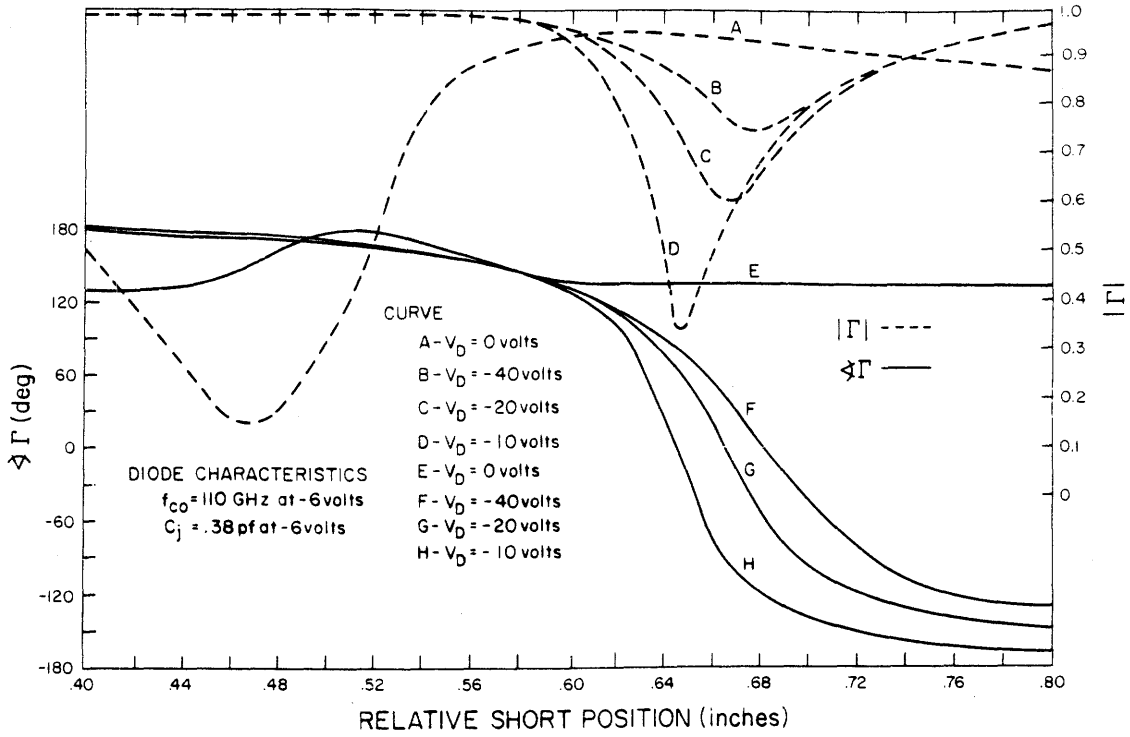

Fig. 6.8 Phase and Magnitude Characteristics of Phase Shifting Element No. 5

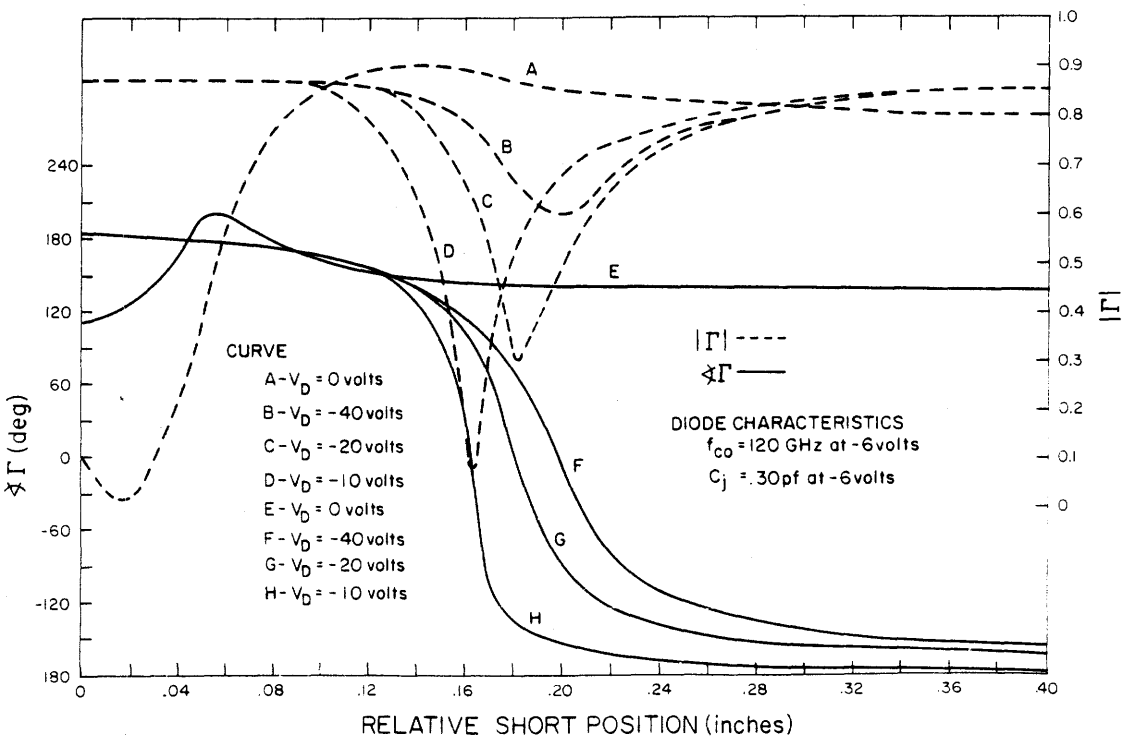

Fig. 6.9 Phase and Magnitude Characteristics of Phase Shifting Element No. 6

resonance. Similar increased losses occur in the other phase shifting elements.

At low bias voltages, the capacitance becomes large enough so that the real part of Z(-a) under parallel resonance conditions is less than the characteristic impedance of the reduced height waveguide. In Chapter II it was predicted that $\sphericalangle\Gamma(-a)$ under these conditions would be 180 degrees instead of 0 degrees and that a slight wiggle in the $\sphericalangle\Gamma(-a)$ curve would occur near this region. The experimental curves show a similar behavior except that the curves, in general, are offset from 180 degrees by varying amounts. This phenomenon is most likely due to small reactances being added by the bias connector in series with the waveguide.

The deviations from the predicted results mentioned above seemed to offer no obvious stumbling blocks to the method of eliminating amplitude modulation mentioned in Chapter II. Therefore, no steps were taken to eliminate these deviations.

CHAPTER VII

PHASE SHIFTER OPERATION

7.1 Phase Shifter Configuration

The six phase shifting elements were connected to three 4-port circulators (as shown schematically in Fig. 1.1) to form the complete phase shifter. The circulators were Melabs Model H-487-243 having at least 20 db isolation between ports 4 and 3 and ports 2 and 1 and at least 40 db isolation between ports 1 and 4 and ports 3 and 2. The high-speed biasing circuits were mounted directly on the diode bias connectors so that there would be no delays or reflections between the biasing circuits and the diodes. Table 7.1 summarizes the operating points and phase increments assigned to the phase shifting elements. As it turned out, the 40 volt biasing circuits were not needed on the 180 and 90 degree phase shifts, but on the 90 and 45 degree phase shifts.

7.2 Switching Speeds and Amplitude Modulation

Transient times of approximately 10 nanoseconds were measured for all but the two smallest phase shifts. The transient times for the two smallest phase shifts could not be measured accurately because of the small output they produced in the phase detector combined with the attenuation of the RF probe which was used to measure the transient times. It is assumed, however, that these transient times were as fast as those for the other phase shifts since the bandwidths of the components in the system impose no greater restrictions on the smaller phase shifts than on the larger phase shifts.

Table 7.1 Phase Shifting Element Operating Points

Phase Shifting Element No.	Assigned Phase Shift	Bias Voltages	Micrometer Dial Setting for Short (Inches)
1	45°	10, 40	.731
2	180°	5, 10	.647
3	$5\text{-}5/8^{\circ}$	17, 20	.740
4	$11\text{-}1/4^{\circ}$	8, 14	.772
5	90°	0, 18	.733
6	$22\text{-}1/2^{\circ}$	0, 2.8	.258

In order to measure the transient times of the phase shifts, it was necessary to use the power limiter discussed in Chapter IV. The power limiter (operating as transmission-type device through the use of a 3-port circulator) was inserted between the output of the phase shifter and the input of the phase detector. This power limiting was necessary so that the rather large amplitude modulation that occured during transients would not affect the output of the phase detector. Figures 7.1 and 7.2 show oscillographs of the phase detector output taken directly from one of the crystal detectors for 180 and 90 degree phase transients. The 180 degree phase transient is shown both with and without limiting. Without limiting, a considerable amount of ringing occurs at the phase detector output. This ringing comes from the transient amplitude modulation which also has the same ringingnature and lasts for about 30 nanoseconds. The ringing in the amplitude apparently comes from the slight amount of ringing present in the bias voltages applied to the diodes. This implies that the amplitude of the phase shifted signal is more sensitive to variations in the diode bias voltage than the phase. This phenomenon was also observed when the phase shifting elements were being adjusted to produce the desired phase increments with as little amplitude modulation as possible other than the transient amplitude modulation.

The bias voltages and short positions of the individual phase shifting elements could be adjusted so that the amplitude modulation on their outputs alone was negligible. However, some coupling existed between the ports of the circulators causing the overall

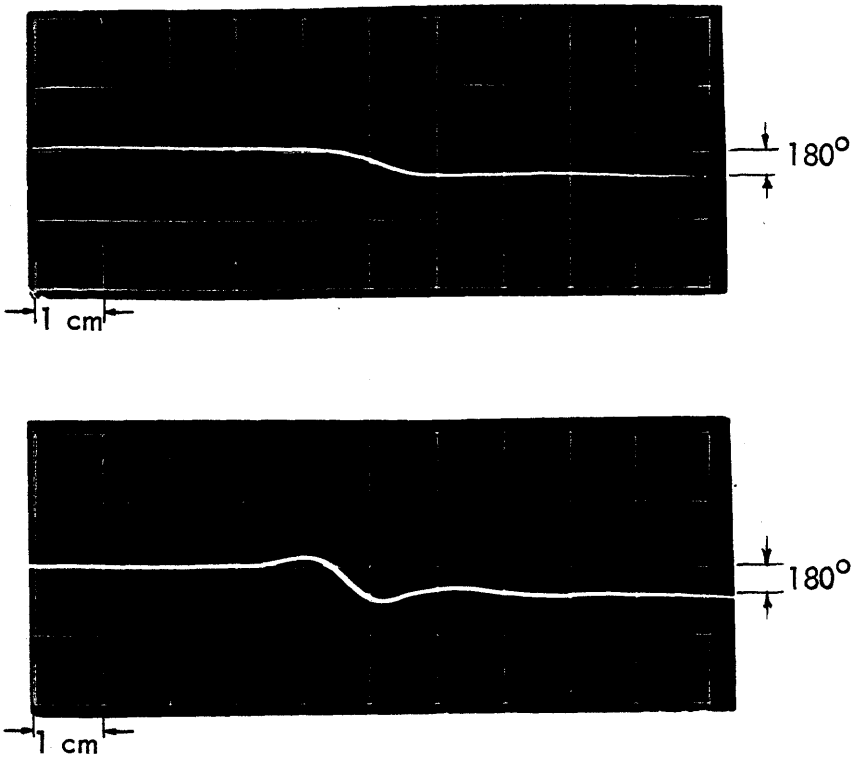

Fig. 7.1 180° Phase Shift. Top: with limiting
Bottom: without limiting. Sweep 10 ns/cm

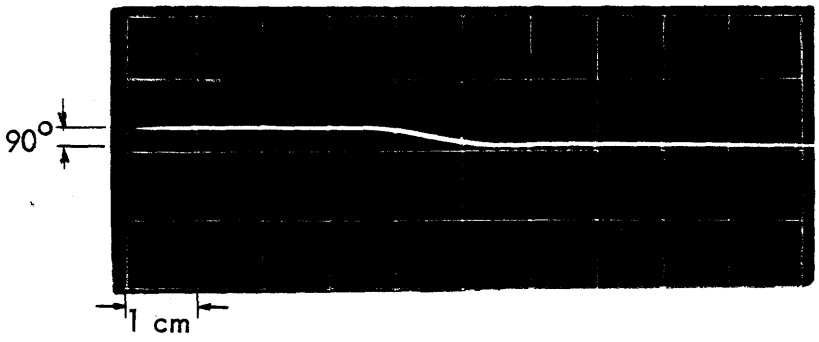

Fig. 7.2 90° Phase shift with limiting
Sweep 10 ns/cm

amplitude modulation to be about 5%. With limiting, this modulation was reduced to 1%. The transient amplitude modulation accompanying the "steady state" modulation amounted to approxima tely 40%. Addition of the limiter reduced this modulation to approximately 20%. The insertion loss of the overall phase shifter was measured to be 13.6 db without the limiter and about 25 db with the limiter.

7.3 Operation with a Binary Counter

A six-bit binary counter was used to control the diode biasing circuits so that the phase output could be incremented cyclically by $\pi/32$ radians. Each counter element controlled one phase shifting element and a variable frequency pulse generator was used to increment the counter. The least significant bit of the counter was used to control the smallest phase shift with the next bit controlling the next larger phase shift and so on up to the most significant bit controlling the 180 degree phase shift. Thus, every time the counter was incremented, the phase shifter would increment the phase by $\pi/32$ radians. After reaching its highest count, the counter would reset by discarding the overflow bit and the phase shifter would have gone through a total phase shift of 360 degrees. In this manner the phase could be incremented continuously and cyclically. The polar plot resulting from feeding the outputs of the phase detector into the x and y inputs of an oscilloscope is shown in Fig. 7.3. Oscillographs of a single output of the phase detector are shown in Fig. 7.4 and 7.5 with two different repetition rates. The frequency of the phase output in Fig. 7.5 is approximately 100 KHz. The noticeable spikes in the phase output at this frequency are due to

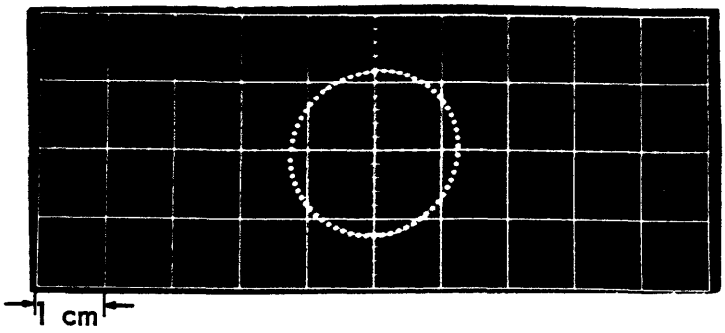

Fig. 7.3 Polar Plot of Phase Detector Output

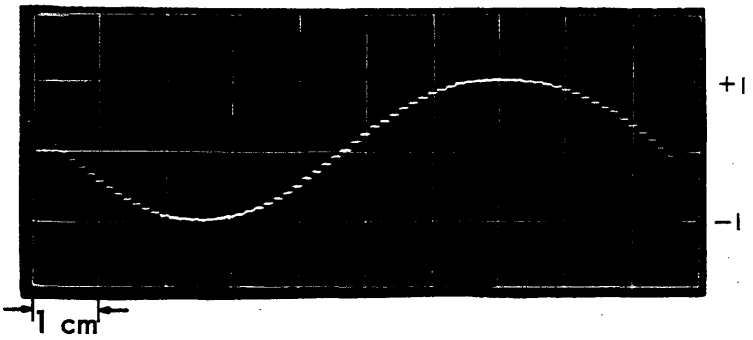

Fig. 7.4 Phase Detector Output. Sweep: 2ms/cm
($\sin\phi$ vs. time)

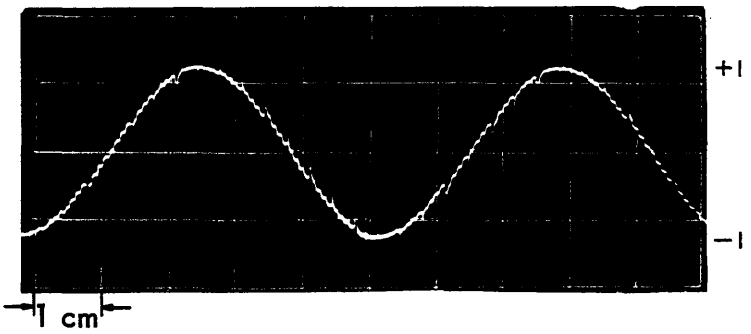

Fig. 7.5 Phase Detector Output. Sweep: 2μs/cm
($\sin\phi$ vs. time)

a combination of the delay in the counter, the transient times of the individual phase shifts not coinciding in the phase shifted signal, and reflections between the phase detector output and the oscilloscope.

7.4 Accuracy

The polar phase plot shown in Fig. 7.3 reveals that the accuracy of the phase shifter for any phase state is close to the design objective of $\pi/64$ radians. It should be pointed out that accuracy depends on how much time one is willing to spend on adjusting the individual phase shifting elements which can be somewhat tedious for the larger phase shifts.

7.5 Conclusions

A phase shifter having 10 nanosecond transient times, 1 percent amplitude modulation (not including transient amplitude modulation) and an accuracy of approximately $\pi/64$ radians has been achieved.

The fact that transient times of less than 10 nanoseconds were not measured, even though four of the biasing circuits could switch in 5 nanoseconds, indicates that bandwidth limitations in the phase shifting elements and in the phase detector were preventing shorter transient times. In the phase shifting elements, a certain amount of energy is stored in the region between the diode and the short so that the transient times can be no shorter than the time it takes for the stored energy to change from one level to another. A similar situation exists in the phase detector, since the 1N23E diodes are mounted in tuned detectors. This effect can be reduced in the phase shifting elements by reducing the volume between the diode and the

shorting plane. A variable short located on the top step of the quarter wave transformer would have greatly reduced this volume and probably would have improved the transient times (assuming the losses in the phase shifting elements remained the same). Unfortunately, time did not permit this idea to be tried, so no supporting experimental evidence can be given.

The 1 percent amplitude modulation accompanying the phase shifts could probably be reduced with better circulators since this modulation was mainly due to cross-coupling of the circulator ports, even though the circulators used were of high quality.

Accuracy better than $\pi/64$ radians could be achieved by spending more effort on the adjustment of the individual phase shifting elements. Cross-coupling of the circulator ports produced no measurable effects on the phase shifts.

The theory set forth in Chapter II proved to be very useful in determining the parameters of the diodes to be used in the phase shifting elements. Equations 2.6 and 2.7 showed the importance of choosing the proper values of L_s and C_j in achieving a parallel resonance condition which is necessary for the larger phase shifts since the phase shifting elements must be operated near parallel resonance to produce these larger phase shifts. The idea of controlling amplitude modulation by appropriately choosing the operating points of the phase shifting elements was also given in Chapter II and proved to be experimentally sound. Although some of the results in Chapter II are not quantitatively correct due to idealization of the situation, they provide a qualitative description of the behavior of the phase shifter and give some physical meaning to this behavior.

REFERENCES

1. Rutz, E.M., and J.E. Dye, "Frequency Translation by Phase Modulation," 1957 IRE WESCON CONV. REC., pt. 1, pp. 201-207.

2. Hardin, R.H., E.J. Downey, and J. Munushian, "Electronically Variable Phase Shifters Utilizing Variable Capacitance Diodes," Proc. IRE, Vol. 48, May 1960, pp. 944-945.

3. Searing, R.M., "Variable Capacitance Diodes Used as Phase Shift Devices," Proc. IRE, Vol. 49, Mar. 1964, pp. 640-641.

4. Cohen, A.E., "Some Aspects of Microwave Phase Shifters Using Varactors," 1962 Proc. 6th Nat'l. Conv. on Military Electronics, pp. 328-332.

5. Garver, R.V., "Broadband Binary 180° Diode Phase Modulators," IEEE Trans. on Microwave Theory and Techniques, Jan. 1965, pp. 32-38.

6. Dawirs, H.N., and W.G. Swarner, "A Very Fast Voltage-Controlled, Microwave Phase Shifter," Microwave J., Vol. 5, June 1962, pp. 99-107.

7. White, J.F., "Semiconductor Microwave Phase Control," NEREM Rec., 1963, pp. 106-107.

8. Marcuvitz, N., Waveguide Handbook, Radiation Laboratory Series, Massachusetts Institute of Technology, McGraw-Hill, New York, 1951.

9. Course notes on "Microwave Circuits," Massachusetts Institute of Technology, 1965, Chapter 3, pp. 10-12.

10. Montgomery, C.G., R.H. Dicke, and E.M. Purcell, Principles of Microwave Circuits, Radiation Laboratory Series, Massachusetts Institute of Technology, McGraw-Hill, New York, 1948.

11. Millet, M.R., "Microwave Switching by Crystal Diodes," IRE Trans. on Microwave Theory and Techniques, July 1958, pp. 284-290.

12. HPA Application Note, "The PIN Diode," Application Note No. 4, Sept. 1964.

REFERENCES (Cont.)

13. Kaiser, J.A., H.B. Smith, W.H. Pepper, and J.H. Little, "An Automatic Microwave Phase Comparator," IRE Trans. on Microwave Theory and Techniques, Nov. 1962.

14. Krupke, D.L., T.S. Hartwick, and M.T. Weiss, "Solid-State X-Band Power Limiter," IRE Trans. on Microwave Theory and Techniques, Nov. 1961

15. Garver, R.V., and D.Y. Tseng, "X-Band Diode Limiting," Correspondence - IRE Trans. on Microwave Theory and Techniques, March 1961, p. 202.

16. Young, L., "Tables for Cascaded Homogeneous Quarter-Wave Transformers," IRE Trans. on Microwave Theory and Techniques, April 1959, pp. 233-237.

17. Handbook of Chemistry and Physics, 41st ed. Chemical Rubber Publishing Co., Cleveland, 1959

18. Ginzton, E.L., Microwave Measurements, McGraw-Hill, New York, 1957